Development of a Contaminant Leaching Model for Aquifer Storage and Recovery Technology

Project Period: 7/2010-6/2012

Reported

by

Abdulwahab M. Ali Tuwati and Maohong Fan*

**PI, SER Associate Professor in the Department of Chemical & Petroleum Engineering*
University of Wyoming
Phone: (307) 766 5633 Email: mfan@uwyo.edu

January 13, 2013

1. ABSTRACT

Wyoming is lacking in water resources. Aquifer storage and recovery (ASR) through water injection could be an important method to solve the water problem in Wyoming. However water injection could lead to contamination of ASR due to the leaching of heavy metals and other elements. Therefore prediction of the potential of leaching of contaminants with a model is critically important to the successes of the application of ASR technology in Wyoming and other states in the US. The proposed project was designed to provide a solution to the universal issue facing many potential ASR technology customers. Both batch leaching and continuous flow leaching tests were conducted under different conditions and the associated leaching models were obtained.

2. INTRODUCTION

The state of Wyoming is considered part of a semi-arid hydro-climatic region, with water levels varying throughout the year due to the warm temperatures and relatively little precipitations. Wyoming is ranked as the third driest state in US, and drought is a constant threat in this region. According to the National Climatic Data Center (NCDC) [1], Wyoming is placed as the 48th wettest in the U.S with annual precipitation average of 12.97 inches. In general, the state has limited sustainable surface water available for use. Furthermore, Wyoming is one of the largest fossil fuel suppliers in the country [1], with large quantities of water generated during production released either onto land or into nearby lakes or rivers with no beneficial use. Worldwide, the oil and gas industry generates more than 70 billion barrels of produced water per year. Within the US alone, between 15 and 20 billion barrels of produced water are generated

each year. This is equivalent to a volume of 1.7 to 2.3 billion gallons per day. Of the above total of produced water, state of Wyoming has shown a share of approximately 2 billion barrels per year as reported in the year 2007 [2]. Accordingly, an environmentally friendly and relatively inexpensive method could be used to store this large volume of the co-produced water after a necessary partial or comprehensive treatment. An aquifer storage and recovery (ASR) injection method could be a feasible technology for conserving natural and/or produced water that would otherwise be wasted. ASR technology provides a cost-effective solution to many of the world's water management needs, storing water during times of flood or when water quality is good, and recovering it later during emergencies or times of water shortage, or when water quality from the source may be poor. Large quantities of water are stored deep underground, which reduces or eliminates the need for construction of large and expensive surface reservoirs. In addition to the abovementioned driving force, ASR technology can also be used to protect environment, aquatic and terrestrial ecosystems. Most ASR storage zones are ranged in depth from 200 to 2,700 ft. Water is stored in different water-bearing geologic formations that may be in sand, clay sand, sandstone, gravel, limestone, dolomite, glacial drift, basalt and other types of geologic settings.

The types of aquifers in North America are generally classified into six groups: unconsolidated and semi-consolidated sand and gravel aquifers, sandstone aquifers, carbonate-rock aquifers, aquifers in interbedded sandstone and carbonate rocks, and aquifers in igneous and metamorphic rocks [3]. Sand and gravel, sandstone, carbonate-rock, and interbedded sandstone and carbonate rock aquifers exist to some extent in the state of Wyoming. Regardless of the aquifer type, the injected "stored" water displaces the natural water that is present in the aquifer and causes a very large bubble around the well. This bubble is usually confined by overlying and underlying geologic formations that do not produce water. These bubbles have water storage

capacities as small as about 13 million gallons in individual ASR wells to as much as 2.5 billion gallons or more in large ASR well fields [4]. However, in order for the ASR to be a successful technology for water storage, potential contamination should be addressed. The contamination might occur during water injection and storage as a result of the leaching of toxic metals.

The present project was designed to study continuous and batch leaching of heavy metals [5] for prediction of the potential leaching of contaminants into aquifers. The effects of varying certain parameters on the mobility of heavy metals through rocks, including pH and temperature, will be studied using both leaching processes. Flow rate was also used as a variable for continuous process studies. This work seeks to study mobility and investigate the leaching kinetics of several heavy metals that may be present in "sandstone" rock types. Sandstones are arenaceous sedimentary rocks composed mainly of feldspar and quartz, and exhibit different colors. They are broadly divided into three groups: arkosic sandstones, which have a high (>25%) feldspar content, quartzose sandstones, such as quartzite, which have a high (>90%) quartz content; and argillaceous sandstones, such as greywacke, which have a significant fine-grained element.

The term "heavy metal" refers to any metallic element that has a relatively high density, and typically refers to the group of metals and metalloids with atomic densities greater than 4 g/cm^3 [6]. Heavy metals are well known to be toxic to human beings and most other organisms when present in high concentrations in the environment [6]. Table 1 lists the standard levels of these elements considered safe in water, according to World Health Organization (WHO) [7] and the United States Environmental Protection Agency (EPA) [8].

Table 1 WHO/EU drinking water standards.

Element	WHO standard (ppb)	EPA standards (ppb)
Arsenic (As)	10.0	10.0
Barium (Ba)	300.0	200.0
Beryllium (Be)	No guideline	4.0
Boron (B)	300.0	N/A
Cadmium (Cd)	3.0	5.0
Chromium (Cr)	50.0	100.0
Copper (Cu)	2000.0	1300.0
Iron (Fe)	No guideline	N/A
Lead (Pb)	10.0	15.0
Manganese (Mn)	500.0	N/A
Nickel (Ni)	20.0	N/A
Selenium (Se)	10.0	50.0
Silver (Ag)	No guideline	N/A
Zinc (Zn)	300.0	N/A

The leaching of heavy metals occurs naturally, as in the case of sulfide minerals in rocks that are oxidized upon contact with water and atmospheric oxygen, resulting in the formation of sulfates that generate so-called “acid rock drainage” and “metal leaching” (ARD-ML). ARD-ML is usually characterized by high concentrations of metals and sulfates in solution and lower pH values (2-4), which leads to the accelerated release of certain metals into aquifers [9-10]. The mobility of arsenic (As) as toxic element in the presence of pyrite in ASR has been reported in various studies as an example of such leaching, and geochemical modeling has examined the stability of pyrite in limestone during the injection into wells of surface water [11]. The goal of those modeling studies was to stabilize pyrite under certain conditions in order to alter the high leaching of As levels into ASRs. Another leaching model investigated interactions among immobilization reactions and transport mechanisms affecting the overall leaching of contaminants [12], and a characteristic leaching procedure for assessing the toxicity of soils

contaminated with heavy metals has been reported elsewhere [13]. In addition, several reports have been cited for the release to groundwater of heavy metals from sources such as fly ash [14], water springs [15], soil [16], mine waste material (i.e., tailings) [17], acidic sandy soil amended with dolomite phosphate rock (DPR) fertilizers [18], and contaminated calcareous soil [15].

All of these reports indicate the mobility of heavy metals in soil to some extent under various amendment conditions. Further, it has been reported that the addition of organic material could result in the fixation of metals such as zinc (Zn) and lead (Pb) in soil, which in turn might help to reduce leaching of these metals into aquifers [19]. The study of metal leaching from various fly ash samples [14] showed different behavior patterns. The chemical partitioning of lead (Pb) and zinc (Zn) in soils, clays and rocks has been documented [17], with their migration showing an increase under low pH conditions. In the present study, we found it both necessary and useful to design and develop leaching models to study the kinetics of each individual contaminant species; to investigate the potential leaching of some of these heavy metals from sandstone rocks using both continuous and batch leaching processes; and to measure the effects of varying parameters such as pH and temperature of the leachate on both leaching processes, as well as the effects of flow rate on the continuous leaching process.

3. METHODS

3.1 Leaching kinetics of heavy metals

Heavy metal leaching models were derived using batch system. Assuming that the leaching of contaminant species, i, follows a first order kinetic model, then its leaching kinetics of can be written as

$$\frac{dC_i}{dt} = k_i[C_{e,i} - C_i] \qquad \text{E1}$$

or

$$-\frac{d[C_{e,i} - C_i]}{dt} = k_i[C_{e,i} - C_i] \qquad \text{E2}$$

where k_i is the leaching rate constant of species *i*, $C_{e,i}$ is the leaching concentration of contaminant *i* at leaching equilibrium state, and C_i is the concentration of species *i* at any time *t*.

With the boundary condition, $C_{i,\,t=0} = 0$, the integral form of E1 is:

$$-\ln\frac{(C_{e,i} - C_i)}{C_{e,i}} = k_i t. \qquad \text{E3}$$

Rearranging E3, we have

$$-\ln[C_{e,i} - C_t] = k_i t - \ln C_{e,i}. \qquad \text{E4}$$

The left side, $-\ln[C_{e,i} - C_t]$ in E4 can be plotted against time (t). If the experimental data fits the plot, then the assumed leaching rate order (1st order) is correct. Otherwise, an alternative leaching rate order needs to be assumed and checked until the experimental data fit the associated kinetic model.

3.2 Experiments

3.2.1 Sample collection and preparation

Sandstone rock samples were collected from an open pit (Figure 1) operated by Black Butte Coal and Mining Company, and located about 170 miles west of Laramie, Wyoming. The samples were obtained from an adjusted depth of about 169 feet to 214 feet, as shown in Table 2.

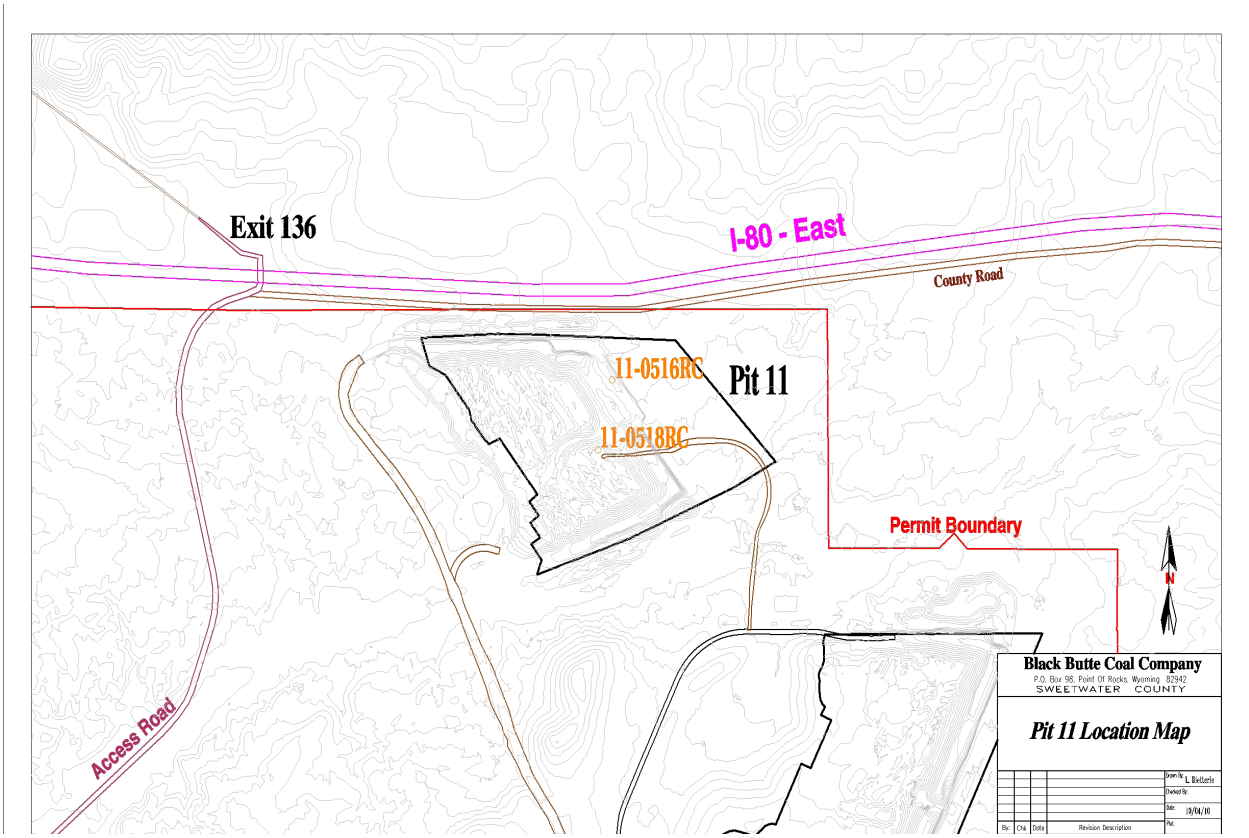

Figure 1. Rock Sample collection location (source: Black Butte Company).

The samples were transported to UW lab in containers, and upon arrival their surfaces were cleaned with water and left to dry at room temperature. After drying, all samples were crushed with a jaw crusher and screened with a sieve (mesh opening of 0.185 inch). The retained particles were then mixed several times to obtain representative samples and kept in closed containers until use.

Table 2 Drill Hole Lithology (Source: Black Butte Company).

Raw depths (feet)	Adjusted depths (feet)	Lithology type	Color
0.00-5.00	0.00-5.05	Soil	Yellowbrown
5.00-22.00	5.05-22.21	Sandstone	Greybrown
22.00-25.00	22.21-25.24	Siltstone	Brown
25.00-29.00	25.24-29.27	Sand	Grey
29.00-56.00	29.27-56.53	Siltstone/mudstone	Grey
56.00-61.00	56.53-61.58	Siltstone	Grey
61.00-74.00	61.58-74.70	Mudstone	Grey
74.00-83.00	74.70-83.78	Siltstone	Grey
83.00-85.00	83.78-85.80	Mudstone	Grey
85.00-93.00	85.80-93.88	Siltstone	Grey
93.00-98.00	93.88-98.92	Mudstone	Grey
98.00-129.00	98.92-130.22	Siltstone	Grey
129.00-135.00	130-22-136.27	Mudstone	Grey
135.00-143.00	136.27-144.35	Siltstone	Grey
143.00-144.00	144.35-145.36	Mudstone	Grey
144.00-150.00	145.36-151.42	Sandstone	Grey
150.00-153.20	151.42-154.65	Mudstone	Grey
153.20-155.00	154.65-156.46	Coal	Black
155.00-158.70	156.46-160.20	Carbonaceous mudstone	Brown
158.70-160.00	160.20-161.51	Coal	Black
160.00-168.00	161.51-169.58	Mudstone	Grey
168.00-212.00	169.58-214.00	Sandstone	Grey
212.00-240.20	214.00-241.20	Coal	Black
240.20-245.00	241.20-245.68	Carbonaceous mudstone	Brown
245.00-247.50	245.68-248.01	Coal	Black
247.50-255.00	248.01-255.00	Sandstone/mudstone	Grey

3.2.2 Sample analysis

An adapted procedure [17] was partially followed for rock sample digestion in order to screen for the following elements: Ag, As, Ba, Be, Cd, Co, Cr, Cu, Mn, Ni, Pb, Se, V and Zn. The first step of the digestion method involved the addition of 5ml aqua regia (1:3 v/v, HNO_3: HCl) and 2 ml hydrofluoric acid (HF) to a 0.2 g fine powder of sandstone rock sample in a Teflon beaker. The sample mixture was then placed on a hotplate and heated at 100°C until dry. Another 5ml of aqua regia was then added to bring the dissolved metals back to the solution. The resulting mixture was then filtered with Whatman 2 filter paper (pore size: 8μm) and rinsed with deionized (DI) water. The filtrate was then transferred into a 50 ml plastic vial and diluted to its mark. The digestion method was performed three times. The final solutions were analyzed by an ICP-OES Spectrometer (ICAP 6000 series, Thermo Scientific).

3.2.3 Leaching apparatus

Two schematic diagrams of continuous and batch percolation extraction set-ups are shown in Figures 2 and 3, respectively; a photo of the actual apparatus (continuous and batch) is shown in Figure 4. The columns are clear PVC columns approximately 7-feet long with an outside diameter (O.D) of 2.5 inches. Each is sufficiently high to contain about 5 kg of rock sample (particle size of 0.185 inch), with additional height to contain applied water in the event of poor percolation. A sampling point at the bottom of the column was used for sampling collection. A cotton filter medium was placed near the sampling point for easy sample withdrawal. Each column has a punch plate and punch plate support, with the bottoms sealed tightly with bubble caps. An adjustable metering pump was used in the continuous leaching

model to ensure a constant flow rate of extraction fluid (water). In the continuous leaching model, containers to hold both influent and effluent liquids were used during extraction.

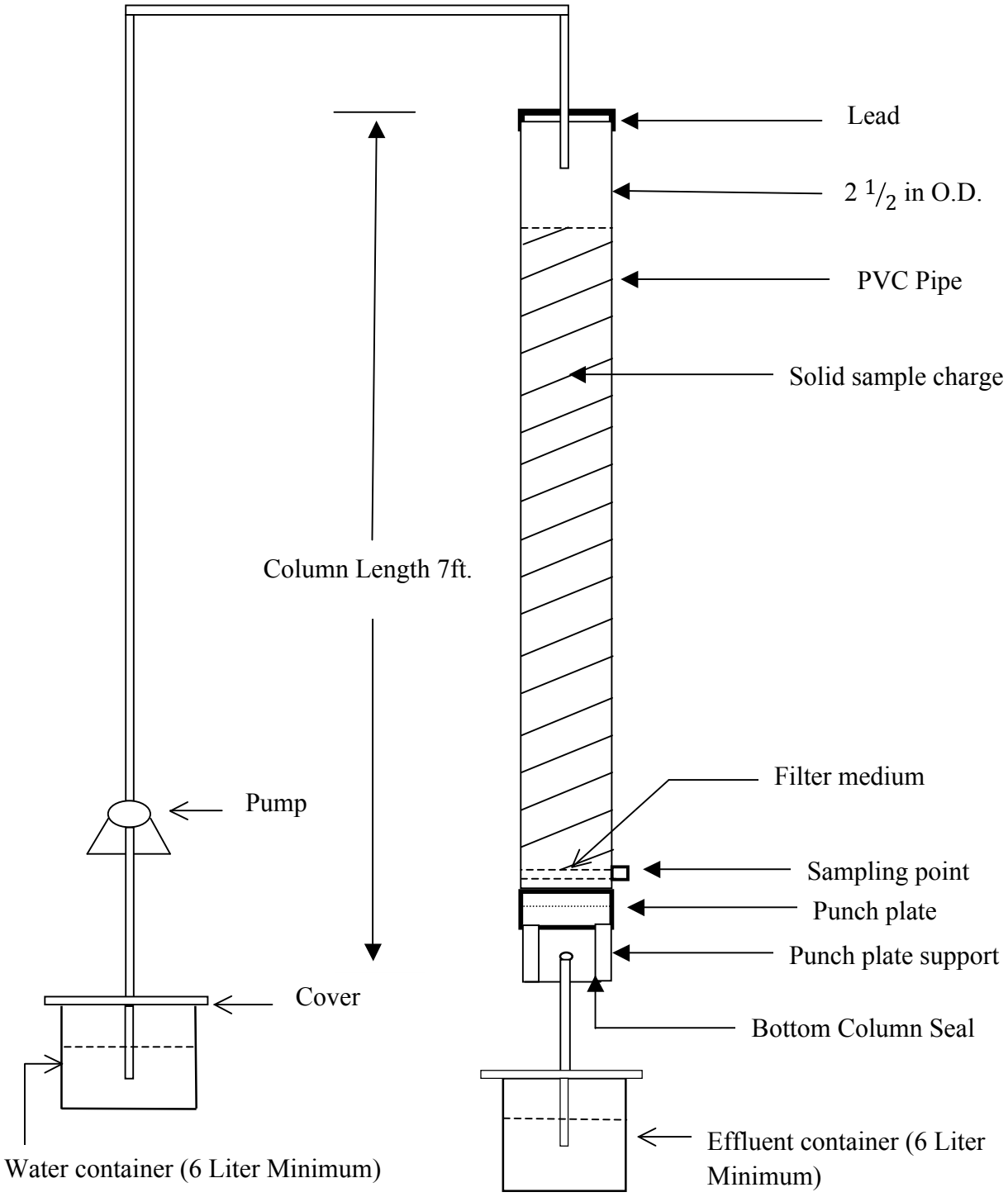

Figure 2 Schematic setup diagram for continuous leaching.

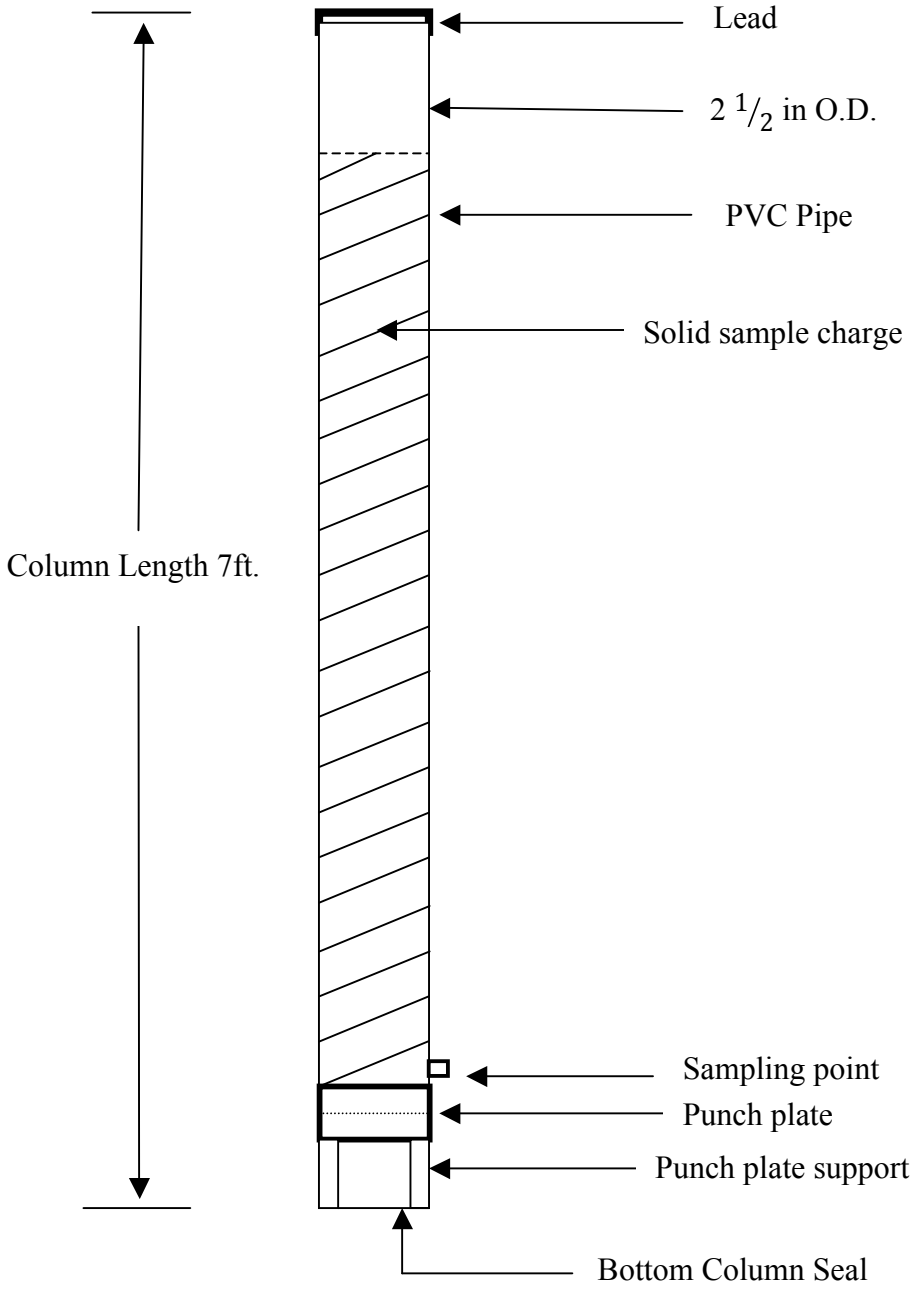

Figure 3 Schematic setup diagram for batch leaching

.

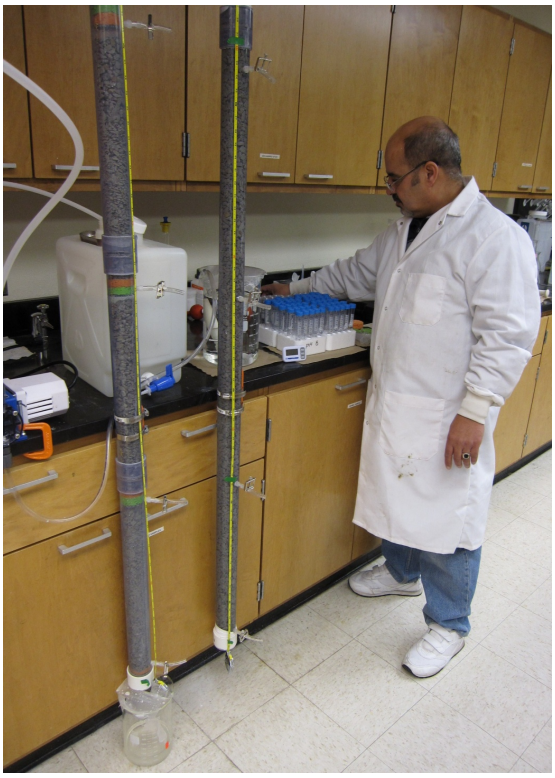

Figure 4 Photo of continuous and batch apparatus.

3.2.4 Operation Procedure

Continuous leaching method

A 5 kg dry rock sample was loaded in increments into the PVC column. In order to minimize particle segregation and compaction, the sample increments were carefully loaded without shaking or tamping. Cotton filter medium was inserted into the column near the sampling point in order to withdraw sample effluents using a syringe during the extraction

process. Deionized water (DI) was pumped from a container holding a minimum of 6 liters into the column at a specified flow rate using a diaphragm-type metering pump (series 100/150). The initial temperature and pH of the leachate water, as well as the date and starting time of the leaching process, were recorded in accordance with ASTM D 1293[19]. Extraction sample of about 10ml was collected in plastic vials from the sampling point at different time periods. Collected leachate samples were then analyzed for leachable metals using an ICP-OES Spectrometer (ICAP 6000 series, Thermo Scientific). The same procedure was used under different experimental conditions, including flow rate and pH.

Batch leaching method

With the exception of the use of a metering pump, a procedure largely similar to method (1) was used to assess the batch leaching method. A set volume of DI water (~1800ml) was added to the column at the start of the leaching process, and small aliquot samples (10ml) were withdrawn and placed into 15 ml vials every 8 hours over a period of 40 hours (unless otherwise specified) from the column sampling point. Procedure was repeated at different pH's and temperatures.

4. FINDINGS/RESULTS AND DISCUSSIONS

4.1 Reference sample analysis

Table 3 lists (in mg/kg) the results of heavy metal concentrations potentially present

Table 3 Metal concentrations in rock sample (sandstone).

Element	Concentration in ppm (mg/Kg)
Arsenic (As)	5.51
Barium (Ba)	206.81
Berillium (Be)	0.93
Cadmium (Cd)	0.85
Cobalt (Co)	4.97
Chromium (Cr)	18.09
Copper (Cu)	8.68
Manganese (Mn)	275.84
Nickel (Ni)	6.19
Lead (Pb)	7.55
Selenium (Se)	5.44
Zinc (Zn)	33.37
Vanadium (V)	38.91

in sandstone rock samples. Because of the chemical composition, matrix complexity, and insolubility of the rock type in mild acidic media (due mainly to a high silica content of approximately 95-97% and various other resistant mineral constituents), the fine powder sample was treated under harsher acidic conditions to ensure complete elemental extraction into the aqueous solution. The method used for the sample dissolution is outlined in section 3.2.2. In order to minimize errors due to the varying distribution of elements within different rocks, the concentrations shown in Table 3 are based on an average of three representative sandstone samples. The reported data are based on the average of three independent runs with a calculated relative standard deviation of ~2%. The sandstone samples were found to contain a total of

thirteen heavy metals at various concentrations, all within the calibration curve and the ICP detectable range. Compared to the remaining elements, barium (Ba) and manganese (Mn) concentration levels were observed to be highest. However, Ba and Mn are considered less harmful contaminants, and their levels in the sample were far below the allowable limits set by the WHO and EPA for standard potable water. Other more toxic elements such as Cd, As, Be, Co, Cu, Ni, Pb and Se were present as well, but with lower ppm-range concentrations. The remaining elements (Cr, Zn and V) showed moderate ppm concentration levels. Iron appeared to be present in high quantities but showed inconsistency (possibly from the jaw crusher's blades) among the samples, so was not included in this study. Actual Fe concentrations will be included in the next report.

In order to get some clue about the chemical composition of the sandstone sample, approximately 4g of finely ground sample was pressed into a solid pellet and scanned by XRF (PANalytical Axios XRF analyzer, PANalytical Inc., Almelo, The Netherlands). Table 4 illustrates the concentrations of some major constituents that are present in the sample. Elements in the actual sandstone rocks are tabulated as "metal oxides" and were reported in weight percent (W %) with absolute errors less than 0.080 percent. It can be seen that, alumina "aluminum oxide" (Al_2O_3) and silica "silicon dioxide" (SiO_2) are predominantly present due to the fact that the rock used in the study is sandstone type. Other metal oxides are present with lower concentrations.

Table 4 The concentrations of major oxides in rock sample (sandstone).

Compound Name	Concentration in weight (%)
Al_2O_3	16.99
BaO	0.07
CaO	3.29
CeO_2	0.02
Cl	0.03
Cr_2O_3	0.01
Fe_2O_3	2.71
K_2O	2.76
MgO	1.55
MnO	0.05
Na_2O	1.12
Nb_2O_5	0.00
NiO	0.01
P_2O_5	1.89
Rb_2O	0.01
SO_3	0.27
SiO_2	68.60
SrO	0.01
TiO_2	0.55
Y_2O_3	0.00
ZnO	0.01
ZrO_2	0.04

4.2 Effect of flow rates on metal leaching

Variations in flow rate were examined in order to determine any effects they might have on the fractionation or the desorption of metals from the sandstone rocks and the dissociation from their counter anions. Aliquots were collected every 8 hours from the column's sampling point over a period of 40 hours and analyzed by ICP. Other experimental parameters such as temperature and pH were kept constant at 21 ^{o}C and 6, respectively. Water was introduced from the top of the column and percolated downward through the sandstone particles at four specified

constant flow rates. The water flow rates used in the study ranged from 11.67 ml/min to 33.33 ml/min. Figures 5 to 9 represent (in ppb) concentrations of soluble metals in the leachate tending toward mobilization through the sandstone particles at various flow rates from the bottom column's sampling point; these were collected at the specified sampling periods.

The results obtained were generated from the average of three independent experiments. Regardless of the flow rate applied, only five of thirteen elements were observed to have any desorption capability through rocks and dissociation from their minerals under the specified conditions. Their easy fractionation might be attributed to their weak physical or chemical adsorption bonding in their minerals, or might instead be due their solubility tendency relative to the other heavy elements.

The majority of the other heavy metals in the studied rock particles did not show any leaching under the given conditions. Their immobility might possibly owe either to their chemical bonding interactions with the rock's particle surfaces or to the formation of complexes with the rock's minerals. Another explanation could be that some might have leached or desorbed out but formed complexes with minerals in the rock and, as a result, showed no solubility toward water. However, as evidenced by its high concentrations at all flow rates and collection times, one of the leached species, boron (B), showed the highest mobility of all the elements. All plots show that concentrations of B exhibited a direct relationship with flow rate, indicating that its migration or desorption increased as it contacted the water flow. By contrast, the fractionation of other leached elements within the run showed somewhat less mobility based on flow-rate variation.

Figures 5 to 9 also show desorption of these metal species with respect to sampling time. It can be observed that prolonged water contact with the particles' surfaces significantly impacted the metals' mobility. Maximum concentration levels of leached metals occurred at the first sampling collection time (8hrs); leachate collected at later sampling times (i.e., 16, 24, 32 and 40 hours) showed lower concentrations of leachable metals. Prolonged contact with the water flow caused desorption within shorter time periods, due either to solubility or the weak physical bonding of these species with the rock surface. It is worth noting that all of the leached metals' concentrations at all flow rates were observed to be below the WHO/EPA drinking water standard limits (Table 1). From these findings, it was determined that to complete the remaining task of determining the effect of pH on metal leaching, a lower flow rate would be recommended in order to minimize desorption of the leachable metals (especially B and Mn).

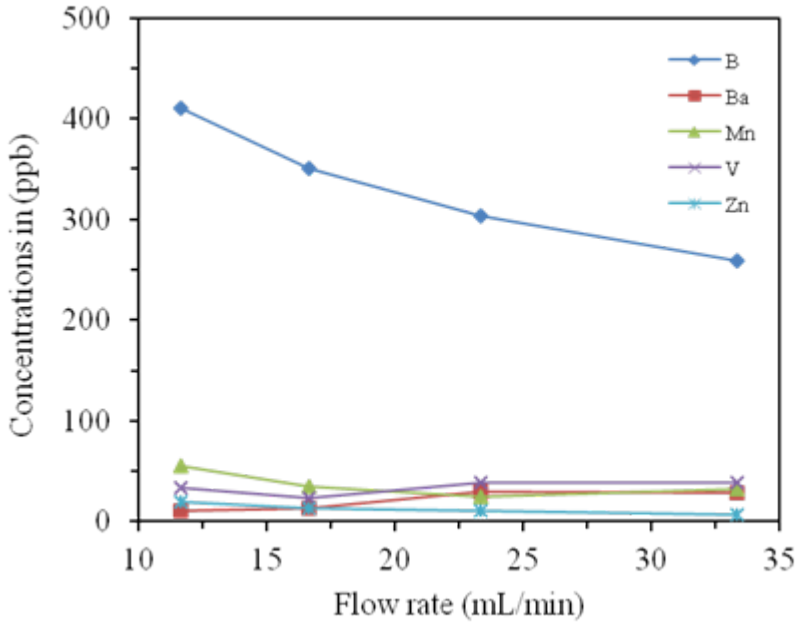

Figure 5 Effect of flow rate on metal leaching (collection time 8 hours).

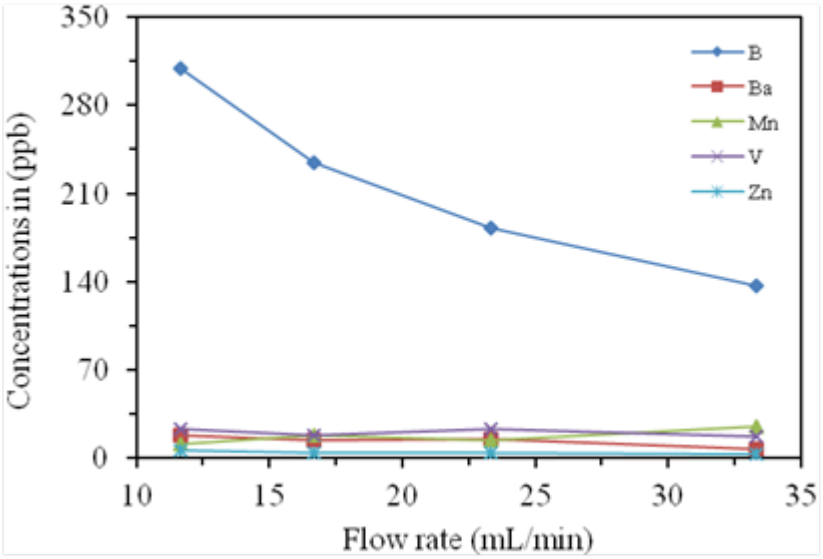

Figure 6 Effect of flow rate on metal leaching (collection time 16 hours).

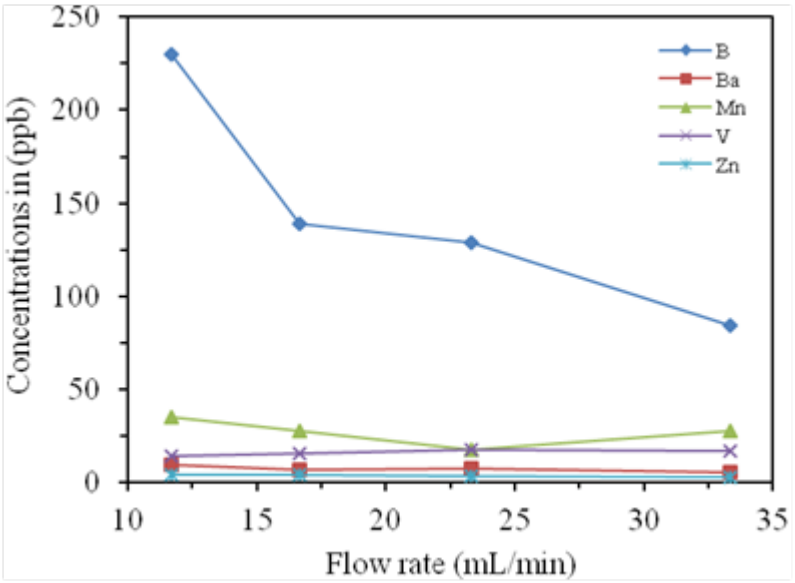

Figure 7 Effect of flow rate on metal leaching (collection time 24 hours).

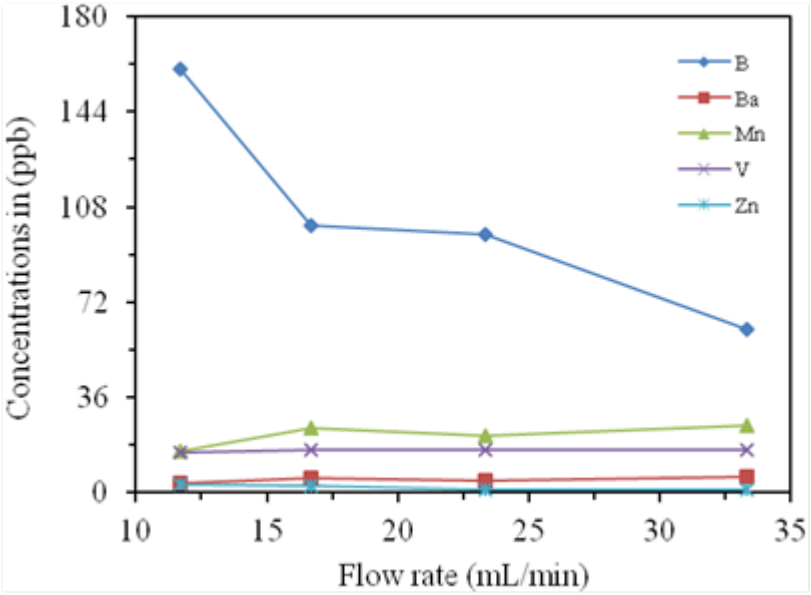

Figure 8 Effect of flow rate on metal leaching (collection time 32 hours).

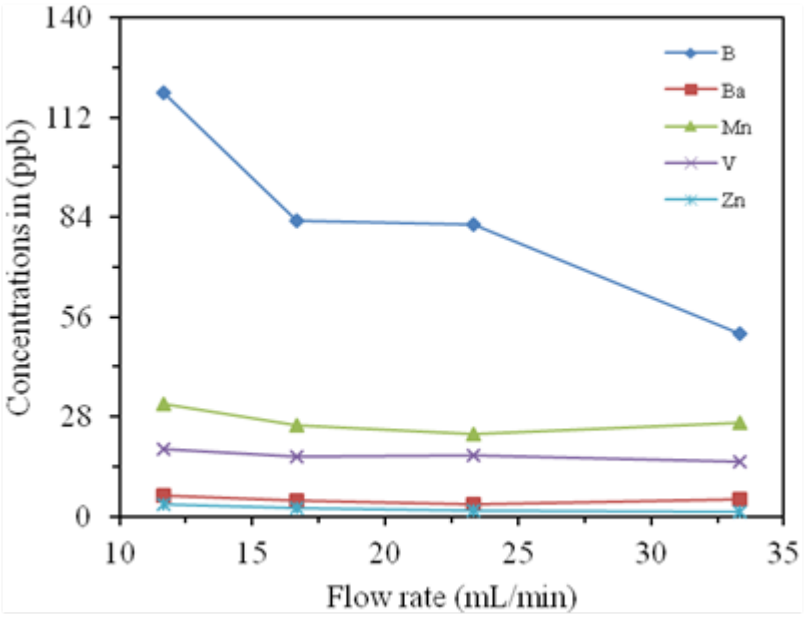

Figure 9 Effect of flow rate on metal leaching (collection time 40 hours).

4.3 Continuous vs. batch leaching

A comparison of continuous and batch processes for the leachable heavy metals is presented in Figures 10 and 11, with levels of the extracted amounts shown in ppb concentrations. The concentrations are plotted against collection sampling time periods of 8, 16, 24, 32 and 40 hours. Experiments were conducted at a constant temperature of 21 ^{o}C and a pH of 6. A water flow rate of 6.33 ml/min was used in the continuous leaching. In the case of batch leaching, a quantity of water (about 1800 ml) was added from the top of the column sufficient to immerse the 5 kg of sandstone particles at the beginning of the process. Samplings were taken periodically every 8 hours. Only four metals (B, Ba, Mn and Zn) appeared to have any mobility in either leaching process. The amounts of Ba and Zn leached were comparable regardless of the leaching process. Steady water contact with the particle surfaces in batch leaching did not cause any noticeable desorption enhancement of the leached metals, rendering extracted metal concentration levels similar to those of the continuous process. However, B was an exception to this finding, evincing a slightly higher mobility in the continuous process compared to the batch process. The reason for this might be due to the flow of water moving downward through the particles, causing the greater mobility of B. By contrast, the behavior of Zn was opposite that of B, due perhaps to the physical interaction or bonding of Zn to the particle surface. Finally, water contact and flow rate were not shown to have any significant effect on leaching of the remaining elements present in the studied rock material. V was not detected as in the previous plots and this could be attributed to the uneven metal's distribution within the rocks.

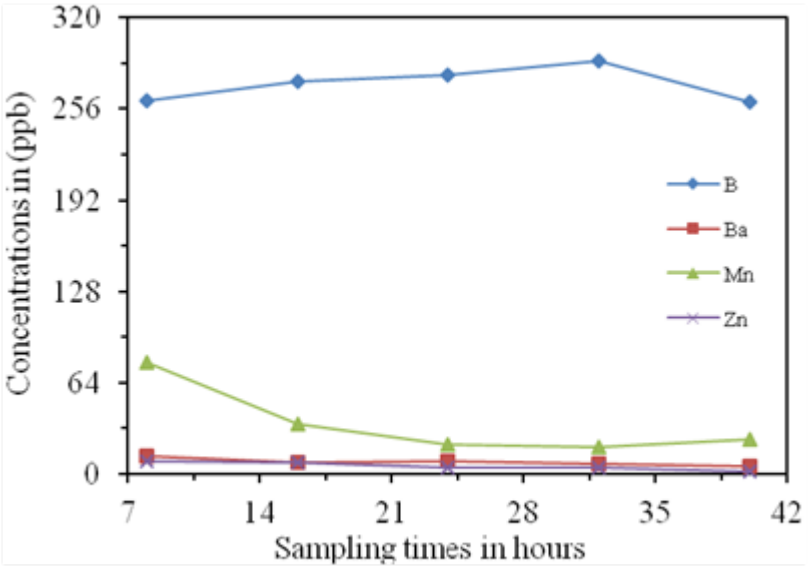

Figure 10 Continuous leaching (flow rate 6.33 ml/min).

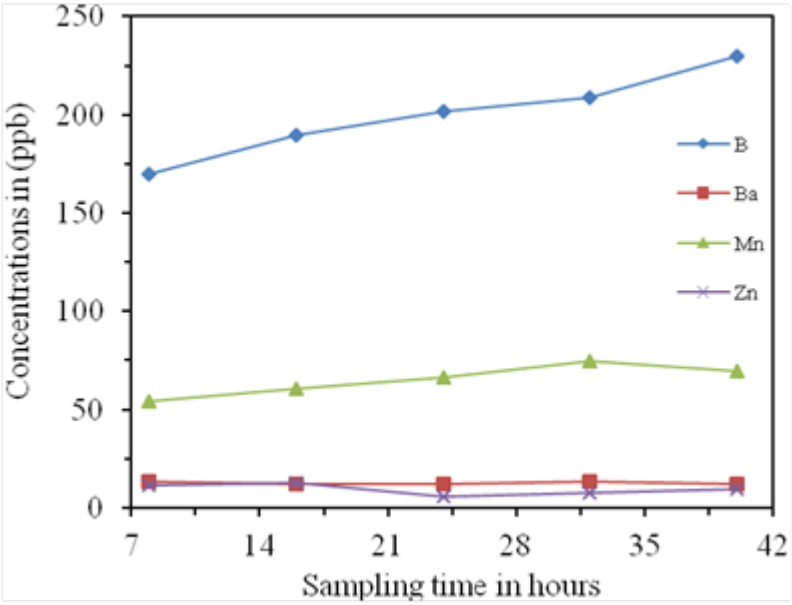

Figure 11 Batch leaching (total volume 1800ml).

4.4 Effect of pH on the heavy metals mobility

Figures 12 to 15 represent leaching of some of the heavy metals that showed their tendency to dissociate or desorb from their minerals and their dependency on pH change. Samples were taken every 12 hours over 10 sampling times. Results obtained in the study showed that only four out of the total thirteen heavy metals present in the sandstone rocks were soluble and fall within the detectable range of ICP calibration curve. These are namely boron, barium, manganese, and vanadium. The concentrations of these cations and their degree of pH dependency have some similar trends. All four metals have a higher solubility at lower pH. An increase in the pH tends to gradually decrease their solubility and as a result they become more immobile and hence less leachable. The lower mobility could be attributed to their precipitations and formation of insoluble (i.e. aluminum oxides or iron hydroxides) complexes in the basic media. Prolonged contact did not seem to cause significant effect on the rate of the dissociation of the metals and particularly in the case Mn and V, whereas B indicated some solubility rate increase with contact time. The solubility profiles are not perfectly graphed which is mainly due to the heterogeneity and the less uniform distribution of the heavy metals within and between the rock samples. Due to the above reason Zn was not present in any of the plots and this could be due to its concentration variation among the rocks or the possibility of its precipitation with iron hydroxides media of higher pH.

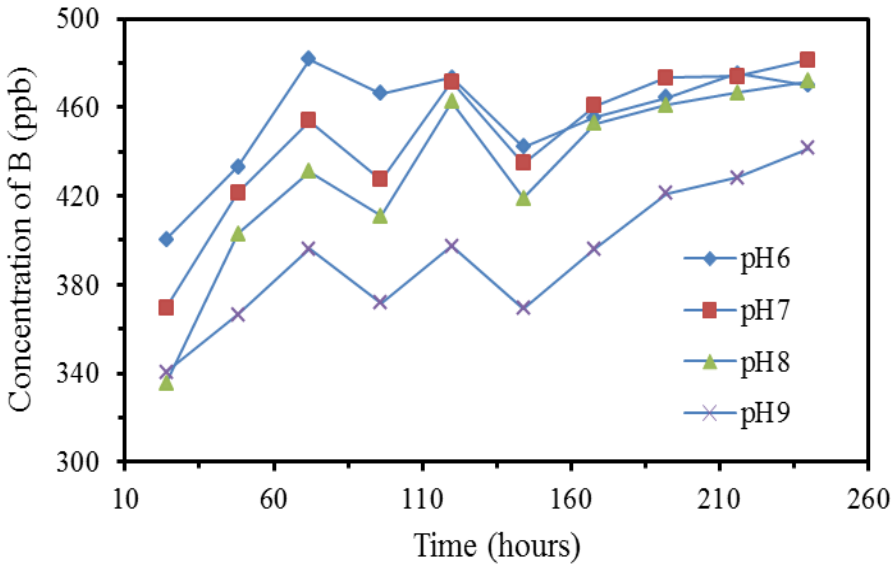

Figure 12 Effect of pH on boron (B) leaching (sampling interval: 12 hours).

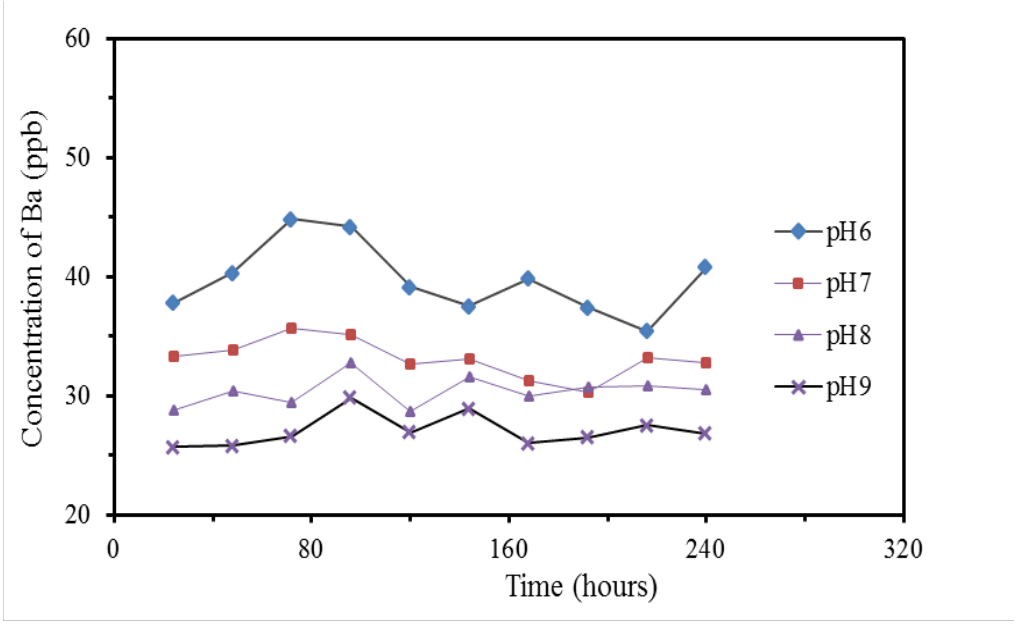

Figure 13 Effect of pH on barium (Ba) leaching (sampling interval: 12 hours).

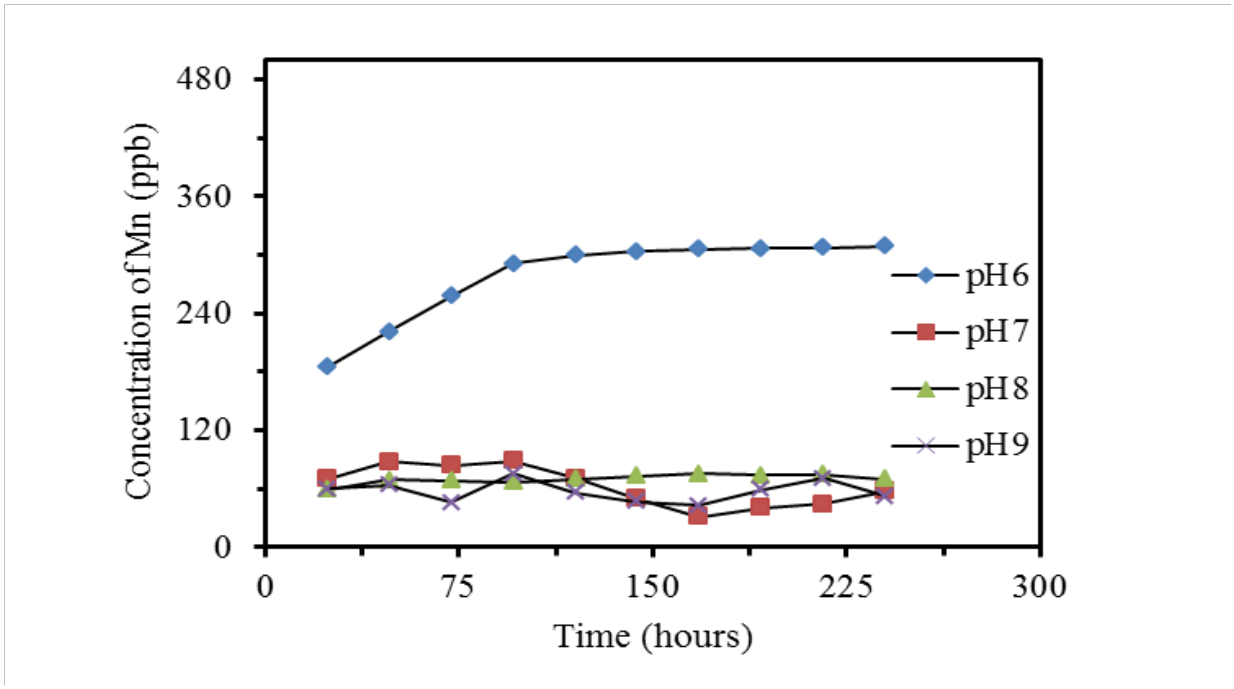

Figure 14 Effect of pH on manganese (Mn) leaching (sampling interval: 12 hours).

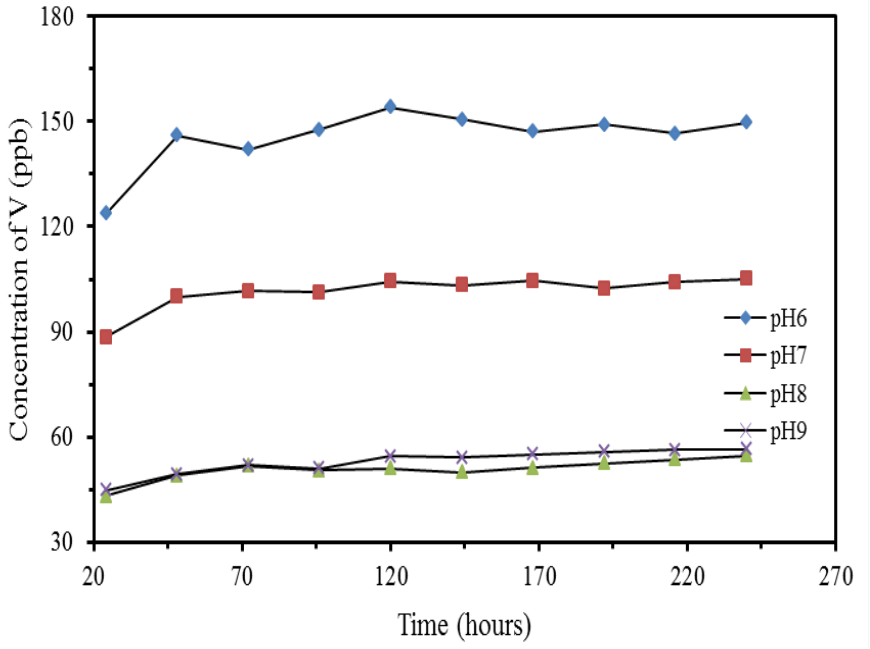

Figure 15 Effect of pH on vanadium (V) leaching (sampling interval: 12 hours).

4.5 Determination of inorganic anions in the leachates

Table 5 lists all possible anions present in the leachate that were collected from the different pH solution media and analyzed via Ion Chromatography (Metrohm 792 IC). In Table 5, sulfate ion has the highest concentrations (441 mg/L to 560 mg/L) among all the anions. This may indicate that most of the leached heavy metal cations originally bonded with sulfate in

Table 5 Anions in leachate.

Sample (mg/L)	pH 6	pH 7	pH 8	pH 9
Fluoride	1.5	1.7	1.7	1.7
Chloride	28.4	29.1	30	45
Nitrite as N	1.7	2.0	0.30	2.2
Nitrate as N	5.7	4.4	4.9	17.4
Bromide	0.2	0.2	0.10	<0.1
Phosphate	<0.1	<0.1	<0.1	<0.1
Sulfate	484	443	441	560

minerals. However, Ba tends to have low solubility in the presence of sulfate which forms BaSO4, but the presence of chloride ion as the second major ion in the leachate (28 mg/L to 45 mg/L) and nitrate ion (4 mg/L to 17 mg/L) would indicate that Ba could be fractionated or desorbed from minerals that contain chloride or nitrates. BaCl2 and Ba(NO3)2 are known to be more soluble, and the presence of high levels of chloride ion may enable sulfate-rich water to retain more Ba in solution. In the case of Mn, it was mentioned that most of its salts are readily soluble in water, with the exception that its carbonate and phosphate have low solubilities in water. Boron salts are generally soluble, although some boron salts such as boron nitrite are completely insoluble in water. Boron halides are soluble in water, which would suggest that

boron could be fractionated or desorbed from chloride mineral complexes. The major anions in the leachate are listed in Table 5.

4.6 Determination of the desorption order of leachable heavy metals

A batch leaching run is presented in Figure 16. Rate of leaching of each individual metal varies with time. B and Mn have similar leaching profiles, where the concentrations show a direct increase with time. Similar leaching behaviors were observed for Ba and V. Leaching rates of Ba an V were almost constant regardless of sampling time. The concentrations of each leached species were plotted against time. If the leaching data of contaminant species *i* fits a first order kinetic model, then plot of $-\ln[C_{e,i} - C_t]$~t should be linear with a high regression coefficient. Figures 17-20 are used to establish the reaction orders of B, Ba, Mn, and V. Generally speaking, the leaching of the four species follows a first order kinetic model. However, the regression values (R^2) for all plots are not very high, which could be attributed to the uneven distribution of heavy metal within the rock particles. Dissociation or desorption rate constant (k_i in E1-E4) for each leached metal can be obtained from the slope of the corresponding plot and they are presented in Table 6.

Table 6 Desorption rate constants (k_i in E1-E4) for leachable metals.

Element	Desorption rate constant [k_i (1/hr) in E1-E4]
Boron (B)	3.68×10^{-2}
Barium (Ba)	3.74×10^{-2}
Manganese (Mn)	3.81×10^{-2}
Vanadium (V)	2.77×10^{-2}

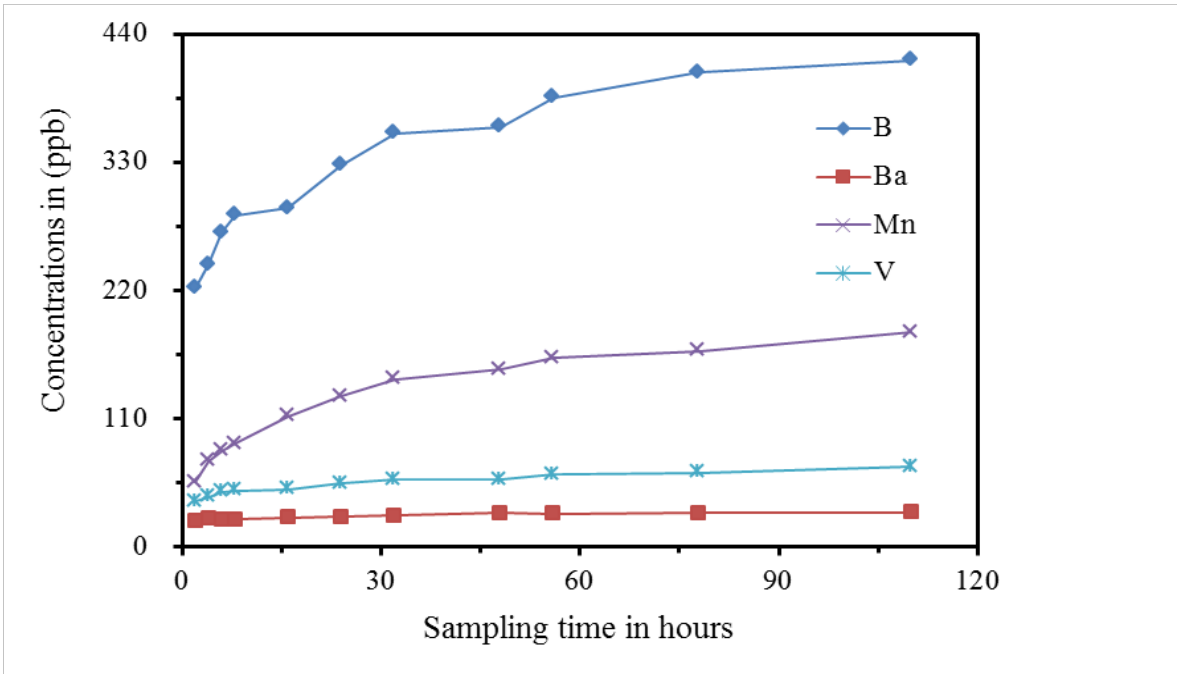

Figure 16 Batch leaching (total volume 2 L).

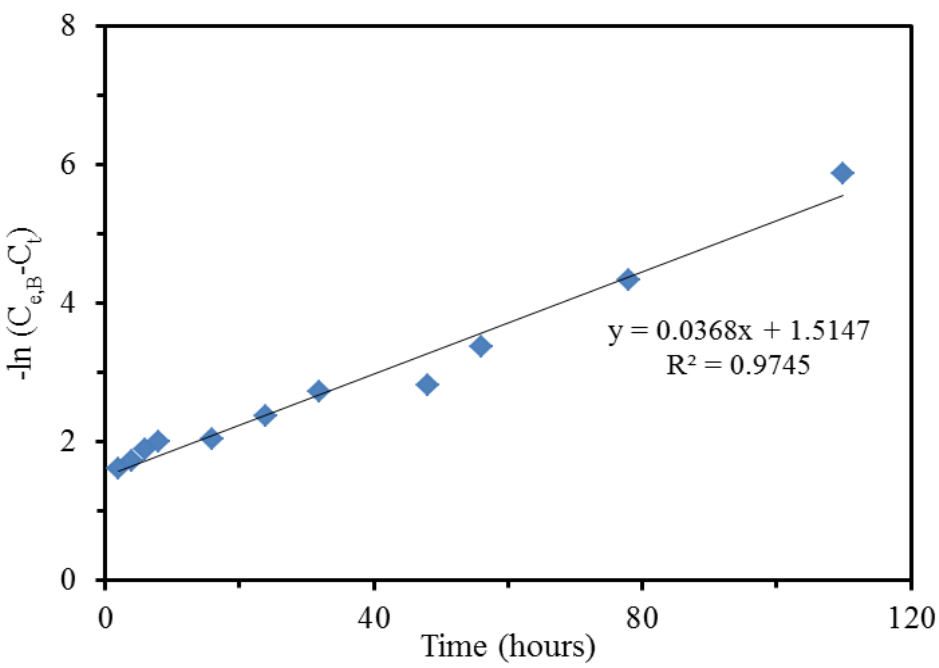

Figure 17 Determination of reaction order of Boron (B).

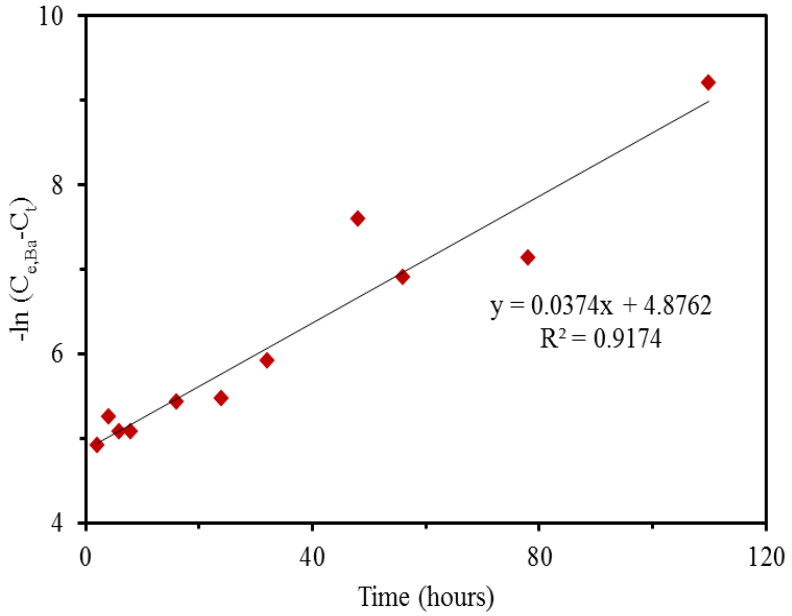

Figure 18 Determination of reaction order of Barium (Ba).

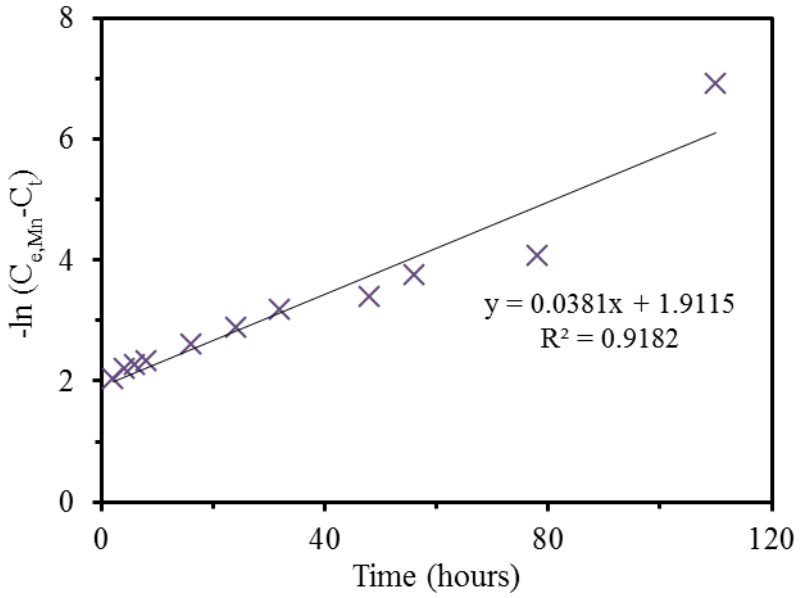

Figure 19 Determination of reaction order of Manganese (Mn).

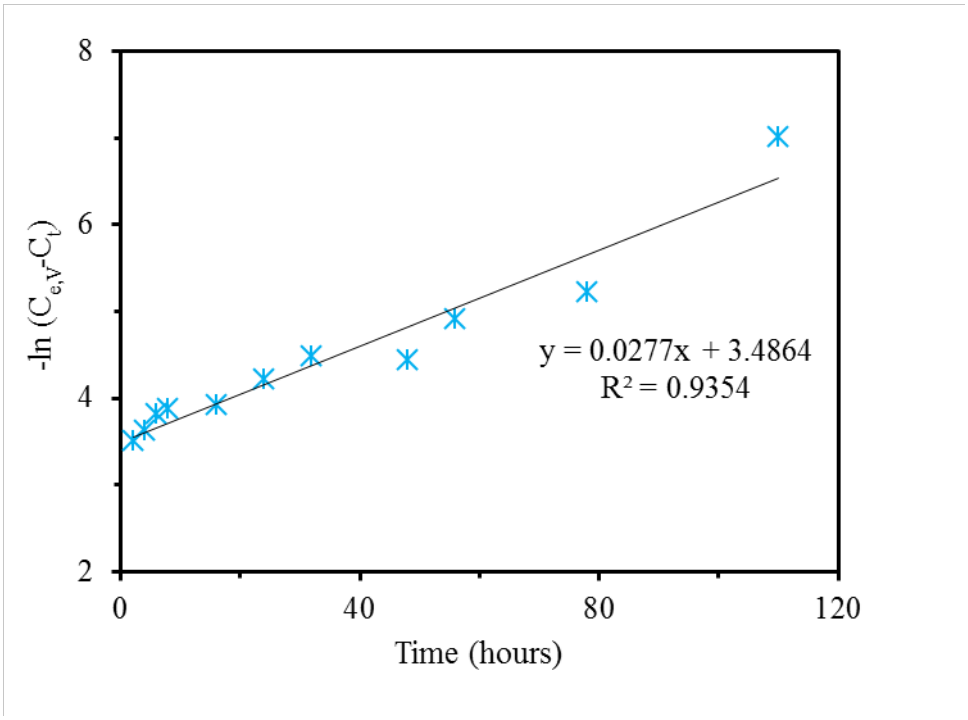

Figure 20 Determination of reaction order of vanadium (V).

4.7 Effect of temperature on the desorption of heavy metals

The depth of an aquifer is another indirect factor to be considered when it comes to the storage of water. Temperature within the Earth increases with depth. It has been reported that the increase is about 25 °C per km of depth in most of the world [19]. As a result it is important to examine the effect of temperature on the desorption of the heavy metals from their minerals. In this study the temperature variations over the range of 5 ^{o}C to 55 ^{o}C were tested to find out their effects on the desorption of the heavy metals. The investigations in this study have shown that only four metals have been desorbed to some degree and dissolved in water regardless of temperature. However, the dissolution of these leached metals has shown an increasing trend with temperature. Tables 7-10 represent the average concentrations of triplicate independent runs

of B, Ba, Mn and V at the specified temperatures. A noticeable increase of the concentration was observed of each metal within each table as going down (as temperature increases) the tables regardless of sampling times. However, the horizontal trend shows no major concentration variations between sampling times, rather a constant rate of leaching and therefore a dynamic status.

Table 7 Boron (B) concentration (ppb).

Day/Temperature (^{o}C)	Day 1	Day 2	Day 3	Day 4	Day 5	Day 6
5	234.4	259.5	215.4	209.9	190.5	211.6
15	252.6	243.8	265.8	248.9	247.4	245.1
25	364.2	379.8	370.9	377.0	379.5	385.5
35	520.2	550.3	583.9	566.7	576.0	606.5
45	671.2	778.5	765.4	795.3	826.0	800.2
55	937.9	966.5	909.4	885.5	897.9	877.9

Table 8 Barium (Ba) concentration (ppb).

Day/Temperature (^{o}C)	Day 1	Day 2	Day 3	Day 4	Day 5	Day 6
5	47.3	38.7	37.8	36.2	39.9	30.0
15	41.6	43.3	41.3	42.9	42.1	40.1
25	51.9	51.0	52.2	49.0	50.1	50.4
35	69.2	67.0	65.7	70.6	65.4	65.3
45	75.4	72.1	73.8	72.1	72.9	70.9
55	89.1	87.2	87.2	86.1	78.4	75.4

Table 9 Manganese (Mn) concentration (ppb).

Day/Temperature (^{o}C)	Day 1	Day 2	Day 3	Day 4	Day 5	Day 6
5	26.6	12.5	9.3	1.7	6.1	6.4
15	4.8	16.8	11.4	9.8	21.6	26.9
25	13.3	32.3	14.3	40.7	60.8	58.4
35	29.7	39.9	78.8	120.7	86.9	68.2
45	41.5	108.3	84.9	124.0	120.9	134.2
55	192.9	252.8	272.6	296.9	291.2	296.1

Table 10 Vanadium (V) concentration (ppb).

Day/Temperature (^{o}C)	Day 1	Day 2	Day 3	Day 4	Day 5	Day 6
5	120.7	117.2	112.0	115.9	107.2	111.1
15	126.2	127.1	138.6	127.6	128.3	128.3
25	150.8	150.3	144.8	143.4	148.2	137.8
35	161.1	149.7	147.5	157.0	149.7	154.6
45	169.5	150.5	153.1	148.7	151.2	151.8
55	159.4	166.6	173.5	165.4	169.6	162.9

4.8 Determination of solubility-product constant, K_{sp}.

The Solubility Product Constant, K_{sp} is the equilibrium constant for a solid substance dissolving in an aqueous solution. It represents the level at which a solute dissolves in solution. This constant can be applied in this study for the leachable metals to check their degree of desorption and hence their solubility in water. The general adsorption/desorption equation of the leaching metals can be written as:

$$M_xA_y(s) \leftrightarrow x\ M^{y+}(aq) + y\ A^{x-}(aq) \qquad R1$$

where $M_xA_y(s)$ represents the undissolved solid or mineral complexes in the rock particle that has shown some tendency to dissolve and dissociate in contact with water to give M^{y+} and A^{x-}. M^{y+} is the leached metal cations such as B, Ba, and Mn dissolved in water. On the other hand A^{x-} is the counter part of the cations (anions listed in table 5). Since the cations and anions concentrations are measured and known, then the equilibrium constants (K_{sp}) for the desorbed species can be found by the following equation:

$$K_{sp} = [M^{y+}]^x[A^{x-}]^y \qquad E5$$

where K_{sp} is the product of the concentration of the ions that are present in the saturated water solution. Tables 11-13 present the K_{sp} values for the data collected at day 6 at temperatures of 5 ^{o}C to 55 ^{o}C for the expected low soluble compounds along with their corresponding literature values. As it can be seen from these tables, the experimental K_{sp} values turned out to be slightly different than that of the ones reported in the literature. The difference may be contributed to the matrix complexity and the chemical composition of the minerals present in the rock. Hence, these metals are not purely dissociated from their counter ions species i.e H^{+}, SO_4^{2-} and OH^{-} , but rather from other minerals. Another reason for this inconsistency could be due to the presence of some precipitating metals or oxides which altered the solubility of these compounds. No K_{sp} values have been found in the literature for Vanadium compounds, as result the experimental Ksp values were not included in the study. Vanadium has been reported to exist as vanadyl and vanadate ions with the chemical formulas (VO^{2+}, $VO(OH)^{+}$) and ($H_2VO^{-}_4$ and HVO^{2-}_2) [20]. These two forms are found to be soluble and easily transfer from geological sediments to water. However, the concentration of vanadium was not high in the water and this is due to the fact that both compound species are known to bind strongly to some minerals and cations and are either adsorbed or form complexes.

Table 11 $B(OH)_3$ solubility product constants.

Temperature (^{o}C)	Conc. Of B (ppb)	Conc. Of $B(OH)_4^{-}$ (mol/L)	Conc. Of H^{+} (mol/L)	Experimental K_{sp}	Literature *K_{sp}
5	211.6	1.9573×10^{-5}	5.0118×10^{-9}	9.8094×10^{-14}	5.80×10^{-10}
15	245.1	2.2671×10^{-5}	5.0118×10^{-9}	1.1362×10^{-13}	5.80×10^{-10}
25	385.5	3.5658×10^{-5}	5.0118×10^{-9}	1.7871×10^{-13}	5.80×10^{-10}
35	606.5	5.6100×10^{-5}	5.0118×10^{-9}	2.8116×10^{-13}	5.80×10^{-10}
45	800.2	7.4017×10^{-5}	5.0118×10^{-9}	3.7096×10^{-13}	5.80×10^{-10}
55	877.9	8.1204×10^{-5}	5.0118×10^{-9}	4.0698×10^{-13}	5.80×10^{-10}

* Literature values at 25 ^{o}C

Table 12 $BaSO_4$ solubility product constants.

Temperature (^oC)	Conc. Of Ba^{2+} (ppb)	Conc. Of Ba^{2+} (mol/L)	Conc. Of SO_4^{2-} (mol/L)	Experimental K_{sp}	Literature *K_{sp}
5	30.0	2.1846×10^{-7}	$5.04x10^{-3}$	$1.1007x10^{-9}$	$1.10x10^{-10}$
15	40.1	2.9200×10^{-7}	$5.04x10^{-3}$	$1.4713x10^{-9}$	$1.10x10^{-10}$
25	50.4	3.670110^{-7}	$5.04x10^{-3}$	$1.8492x10^{-9}$	$1.10x10^{-10}$
35	65.3	$4.7551x10^{-7}$	$5.04x10^{-3}$	$2.3958x10^{-9}$	$1.10x10^{-10}$
45	70.9	$5.1629x10^{-7}$	$5.04x10^{-3}$	$2.6013x10^{-9}$	$1.10x10^{-10}$
55	75.4	$5.4905x10^{-7}$	$5.04x10^{-3}$	$2.7664x10^{-9}$	$1.10x10^{-10}$

*Literature values at 25 ^oC

Table 13 $Mn(OH)_2$ solubility product constants.

Temperature (^oC)	Conc. Of Mn^{2+} (ppb)	Conc. Of Mn^{2+} (mol/L)	Conc. Of OH^- (mol/L)	Experimental K_{sp}	Literature *K_{sp}
5	6.4	1.1650×10^{-7}	1.9952×10^{-6}	4.6377×10^{-19}	1.9×10^{-13}
15	26.9	4.8964×10^{-7}	1.9952×10^{-6}	1.9493×10^{-18}	1.9×10^{-13}
25	58.4	1.0630×10^{-6}	1.9952×10^{-6}	4.2319×10^{-18}	1.9×10^{-13}
35	68.2	1.2414×10^{-6}	1.9952×10^{-6}	4.9421×10^{-18}	1.9×10^{-13}
45	134.2	2.4428×10^{-6}	1.9952×10^{-6}	9.7248×10^{-18}	1.9×10^{-13}
55	296.1	5.3897×10^{-6}	1.9952×10^{-6}	2.1457×10^{-17}	1.9×10^{-13}

*Literature values at 25 ^oC

4.9 Determination of enthalpies (ΔH) and entropies (ΔS) for the leachable elements

Determination of the thermodynamic quantities, i.e ΔH and ΔS, for the leachable elements can be obtained by measuring K_{sp}, over a specified temperature range. These thermodynamic quantities can be expressed by the following equation as;

$$\Delta G^\circ = \Delta H^\circ - T\Delta S^\circ \qquad \text{E6}$$

where ΔG, is the free energy change in a reaction. It can also be related to K_{sp} for the reaction by the equation,

$$\Delta G^\circ = -RT \ln(K_{sp}) \qquad E7$$

Substitution of the left side of E6 with the right side of E7 yields E8.

$$-RT\ln(K_{sp}) = \Delta H^\circ - T\Delta S^\circ \qquad E8$$

Rearrangement of E8 can lead to the following form, E9;

$$\ln(K_{SP}) = -\frac{\Delta H^\circ}{R}\frac{1}{T} + \frac{\Delta S^\circ}{R} \qquad E9$$

Equation E9 is well suited for finding ΔH° and ΔS° by linear regression. Plotting Ln (K_{sp}) vs. 1/T as illustrated in Figures 21-23 would give the quantities of ΔH° and ΔS° from slopes (m = - ΔH°/R) and intercepts (b = ΔS°/R). The experimental thermodynamic values ΔH°, ΔS° and ΔG° for each leachable species are presented in Table 14.

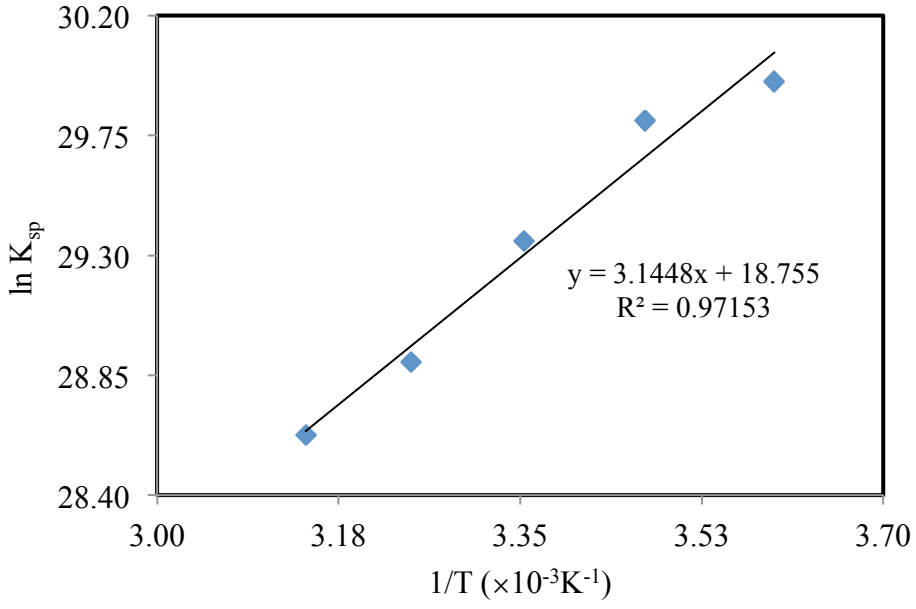

Figure 21 Determination of enthalpy and entropy of $B(OH)_3$.

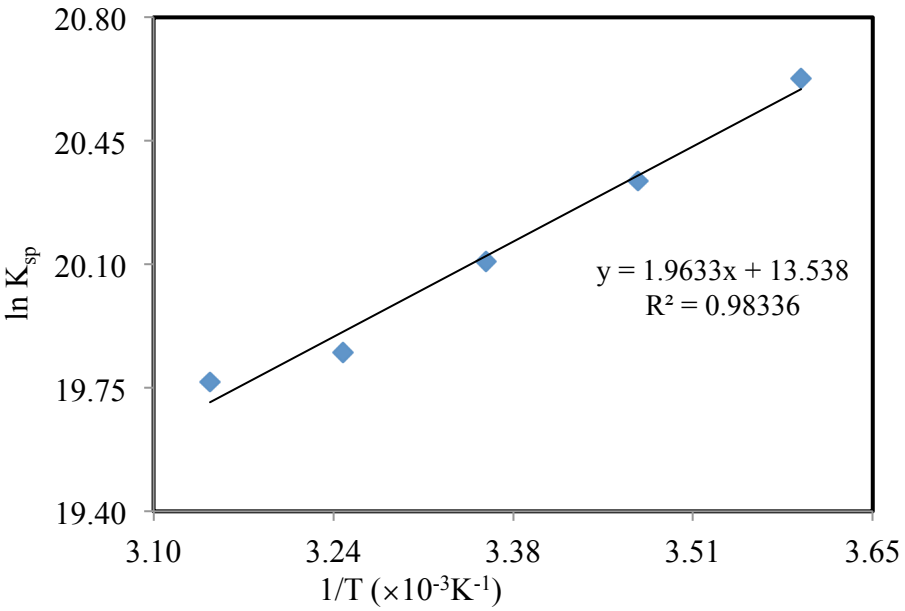

Figure 22 Determination of enthalpy and entropy of $BaSO_4$.

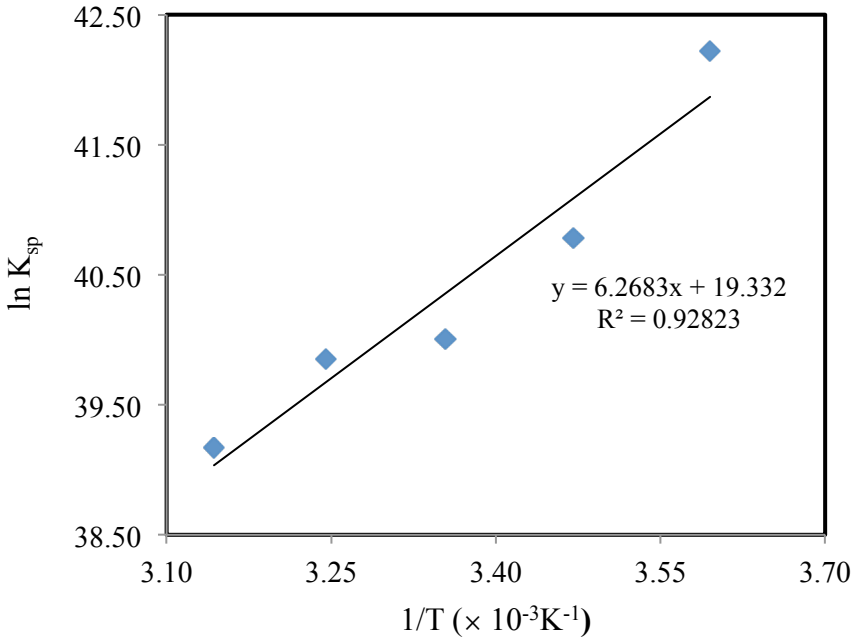

Figure 23 Determination of enthalpy and entropy of $Mn(OH)_2$.

Table 14. Leachable metals thermodynamic values ΔH°, ΔS° and ΔG°.

Compound	ΔH° [KJ/mol]	ΔS° [KJ/(K·mol)]	ΔG° [KJ/mol]
$B(OH)_3$	26.15	155.93	-20.34
$BaSO_4$	16.32	112.55	-17.23
$Mn(OH)_2$	52.12	160.74	41.93

5. CONCLUSIONS

Contaminant leaching model for aquifer storage and recovery technology (ASR) has been investigated in this study. The first part of the study was focused on a number of factors that could contribute or enhance the mobility of metals. These factors included pH, water injection flow rate, and temperature variation. The second part of the study examined the kinetic and thermodynamic properties of the leachable metals. The fractionation or the desorption of the leached metals from the studied sandstone rock samples were examined under the above mentioned conditions. However, only four metals out of the fifteen initially present in the rock samples desorbed and appeared to show minimal concentrations in the water leachate compared to that of reference samples. These concentrations were also found to be significantly below the WHO/EU standard limits for drinking water. Due to the very small contaminants found in the leachate, this puts the ASR as a promising and an alternative technology that would be used as way to replace some other more expensive methods such as surface reservoirs.

6 PROJECT PUBLICATIONS AND PRESENTATIONS

1. Abdulwahab Tuwati, Environmental Issues and Their Solutions Associated with Fossil Fuel Energy Production, PhD Dissertation, Department of Chemistry, University of Wyoming, Laramie, WY.
2. Sharrad, M. O., Liu, H., and Fan, M. (2012), "Selenium Removal from Water by FeOOH," Separation and Purification Technology, Vol. 84, No. 1, PP. 29-34.
3. Presentations
    a. Wyoming Water Research Program, Thursday, December 2, 2010, in the WWDC conference room, 6920 Yellowtail Rd, Cheyenne
    b. Department of Chemistry at University of Wyoming, December 8, 2010.

7 STUDENT SUPPORT AND TRAINING

1. Abdulwahab Tuwati, Department of Chemistry, University of Wyoming
2. Mustafa Sharrad, Department of Chemical & Petroleum Engineering, University of Wyoming
3. Mohamad Rizan Fazily, Department of Chemical & Petroleum Engineering, University of Wyoming
4. Andrew Thomas Jacobson, Department of Chemical & Petroleum Engineering, University of Wyoming

8 REFERENCES

1. I. McBeth, K. J. Reddy, Q. D. Skinner, Chemistry of trace elements in coalbed methane product water, Water Research, 37(2003) 884-890.
2. Nevada Mining Association (1996), Meteoric Water Mobility Procedure, *Standardized Column Percolation Test Procedure*, Nevada Mining Association, Reno, NV, 5p. http://ndep.nv.gov/bmrr/mobilty1.pdf.
3. R. B. Lai, Effect of heavy metal toxicity and exposure on human health, Indian Journal of Environment and Ecoplanning, 2(2005) 533-536.
4. Water Treatment Solutions, Lenntech. WHO/EU drinking water standards comparative table, http://www.lenntech.com/who-eu-water-standards.htm.
5. Drinking Water Contaminants, National Primary Drinking Water Regulations, http://water.epa.gov/drink/contaminants/index.cfm.
6. K. A. Mortin, N. M. Hutt, Environmental geochemistry of mine site drainage: Practical and case studies. Minesite Drainage Assessment Group (MDAG) Publishing, (1997) 333.
7. J. G. Skousen, Acid mine drainage, Acid Mine Drainage Control and Treatment: West Virginia University and National Mine Land Reclamation center, 91(1995) 12.
8. W. Gregg, P. Thomas, Relationship between pyrite stability and arsenic mobility during aquifer storage and recovery., Environmental Science & Technology, 41(2007) 723-730.
9. B. Batchelor, Leach models for contaminants immobilized by pH-dependent mechanisms, Environmental Science & Technology, 32(1998) 1721-1726.
10. Y. Sun, Z. Xie, J. Xu, Z. Chen, R. Naidu, Assessment of toxicity metal contaminated soils by the toxicity characteristic leaching procedure, Environmental Geochemistry and Health,

28(2006) 73-78.

11. B. Ludwig, P. Khanna, J. Prenzel, F. Beese, Heavy metal release from different ashes during serial batch tests using water and acid, Waste Management, 25(2005) 1055-1066.
12. A. Batayneh, Heavy metals in water springs of the Yarmouk Basin, North Jordan and their potentiality in health risk assessment, Internal Journal of Physical Science, 5(2010) 997-1003.
13. K. M. Banat, F.M. Howari, A.A. Al-Hamad, Heavy metals in urban soils of central Jordan: Should we worry about their environmental risks? Environmental Research, 97(2005) 258-273.
14. B. A. Mendez-Ortiz, A. Carrillo-Chavez, M. G. Monroy-Fernandez, Acid rock drainage and metal leaching from mine waste material (tailings) of Pb-Zn-Ag skarn deposit: environmental assessment through static and kinetic laboratory tests, Revista Mexicana de Ciencias Geologicas, 24(2007) 161-169.
15. G. C. Chen, Z. L He, P. J. Stoffella, X. E. Yang, S. Yu, J. Y. Yang, D. V. Calvert, Leaching potential of heavy metals (Cd, Ni, Cu and Zn) from acidic sandy soil amended with dolomite phosphate rock (DPR) fertilizers, Journal of Trace Elements in Medicine and Biology, 20(2006)127-133.
16. R. Clemente, A. Escolar, M. P. Bernal, Heavy metals fractionation and organic matter mineralization in contaminated calcareous soil amended with organic materials, Bioresource, 97(2006) 1894-1901
17. J. E. Maskall, I. Thornton, chemical partitioning of heavy metals in soils, clays and rocks at historical lead smelting sites, Water, Air, and Soil Pollution, 108(1998) 391-409.
18. M. Bettinelli, U. Baroni, N. Pastorelli, Analysis of coal fly ash and environmental materials

by Inductively Coupled Plasma Atomic Emission Spectrometry: comparison of different decomposition procedures, Journal of Analytical Atomic Spectrometry, 2(1987) 485-489.

19. MadScience Network: Earth Sciences, www.madsci.org/posts/archives/200203/1017275290 .Es.r.html.
20. W. Bernhard, S. Werner, Vanadyl in natural waters: Adsorption and hydrolysis promote Oxygenation, Geochimica et Cosmochimica Acta, 53(1989) 69-77.